2.N

Nuclear Physics A266 (1976) 215—227; © *North-Holland Publishing Co., Amsterdam*

EVIDENCE FOR INELASTIC PROCESSES IN THE $^{24}Mg(^{13}C, ^{12}C)^{25}Mg$ REACTION AT E_{lab} = 30 MeV

N. E. SANDERSON

Physics Department, University of Birmingham, Birmingham B15 2TT, England

and

M. IVANOVICH

Nuclear Physics Division, AERE, Harwell, Oxfordshire OX11 ORA, England

Received 22 March 1976

Abstract: The $^{24}Mg(^{13}C, ^{12}C)^{25}Mg$ reaction has been studied at 30 MeV using a magnetic spectrometer. Differential cross sections for transitions to several final states in ^{25}Mg have been measured and analysed using an exact finite range DWBA code. The DWBA predictions have fitted the bell-shaped distributions satisfactorily, yielding spectroscopic factors which are in reasonable agreement with those obtained using (d, p) reactions. The exceptions are the $\frac{3}{2}^+$ state at 0.97 MeV which displays a marked departure from the bell-shaped angular distribution obtained for the other $\frac{3}{2}^+$ state at 2.80 MeV, and the $\frac{7}{2}^+$ state at 1.61 MeV whose angular distribution has an unusual shape, displaying a deep minimum located at the grazing angle. A semi-quantitative model has been used to suggest that the angular distribution for the 0.97 MeV state is evidence for the coupling of inelastic processes in this transition. In the case of the 1.61 MeV state it is suggested that the angular distribution shows the influence of indirect Coulomb excitation on the transfer cross sections.

E

NUCLEAR REACTIONS $^{24}Mg(^{13}C, ^{13}C)$, $E = 30$ MeV; measured $\sigma(\theta)$. ^{24}Mg $(^{13}C, ^{12}C)$, $E = 30$ MeV; measured $\sigma(E_{12C}, \theta)$. ^{25}Mg levels deduced spectroscopic factors. DWBA analysis. Enriched targets.

1. Introduction

The semi-quantitative model of Kahana *et al.* [1]) which is an extension of earlier treatments of heavy ion induced reactions by Strutinskii [2]) and Frahn and Venter [3]), leads to a simplified explanation of the variation in the shape of angular distributions from smooth bell-shaped to oscillatory patterns. This change-over can occur either because of an increased localization in l-space [4]), or because of raising the bombarding energy sufficiently high above the Coulomb barrier [5]) in which case oscillations first appear forward of the grazing peak [6]). The model also explains the circumstances under which a dependence on the L-transfer can occur in the most forward peak of the distribution [7, 8]).

Within the framework of the single-step DWBA formalism all of the above general features can be predicted. One surprising result has been the rather shallow absorptive

potentials necessary to reproduce the forward angle cross sections [9]). Angular distributions measured at reasonably low energies ($\lesssim$ 1.5 times the Coulomb barrier) have proved to be particularly sensitive to this part of the potential [9]). However, in single-nucleon transfer studies problems encountered with DWBA include predicted oscillations which are out of phase with the data [10]) and the necessity of adjusting optical model parameters to fit different final states in a given reaction [11]). Of particular interest to the present work is a report of some (^{16}O, ^{15}N) reactions on s-d shell targets at 45 MeV bombarding energy by Ball *et al.* [12]), where forward of the grazing peak the angular distributions showed a rather smooth and pronounced increase to forward angles, in marked contrast to the DWBA predictions. The influence of multi-step processes is obviously a possibility to be considered especially for reactions carried out on highly deformed nuclei in the s-d shell. The presence of such processes has recently been demonstrated in a number of two-nucleon transfer reactions [see for example refs. [13, 14])].

To investigate some of these discrepancies we have measured differential cross sections for transitions to several states in ^{25}Mg using the ^{24}Mg(^{13}C, ^{12}C) reaction at an incident energy of about 25 % above the Coulomb barrier. Thus, a range of excitations and L-transfers was available for study. This reaction was also chosen because of the highly deformed nature of both the target and the residual nucleus. Multistep contributions were found to be non-negligible in the ^{24}Mg(d, p)^{25}Mg reaction [15, 16]) and it was of interest to see if they announced themselves in any significant way in the present case.

2. Experimental method and results

A 30 MeV ^{13}C beam from the Harwell Tandem accelerator was used to bombard ^{24}Mg (99.9 % enriched) targets of 100 $\mu g \cdot cm^{-2}$ thickness. The targets were either evaporated on 10 $\mu g \cdot cm^{-2}$ carbon backing, or rolled, self-supporting foils. The reaction products were detected using two 5 cm long solid-state position sensitive detectors placed side by side in the focal plane of a Buechner magnetic spectrograph. The energy and position signals were processed by Harwell 2000 series electronics, digitised and recorded on magnetic tape in an event-by-event mode [17]). The two signals were used to derive a mass identification function proportional to Q^2/M for each ion, as well as the radius of curvature, and hence the momentum in the magnetic field. Thus, it was possible to separate clearly the ^{12}C(6^+) ions from elastically scattered ^{13}C(6^+) ions. The highly negative Q-value for the (^{13}C, ^{12}B) reaction ensured that ^{12}B(5^+) ions were far removed on the focal plane. A typical position spectrum for ^{12}C(6^+) ions from the ^{24}Mg(^{13}C, ^{12}C)^{25}Mg reaction is shown in fig. 1. The equivalent energy resolution for the levels of the residual nucleus is about 140 keV FWHM. The peaks in the spectrum have been identified with the known levels in ^{25}Mg [ref. [18])]. Levels at 2.74 MeV ($\frac{7}{2}^+$) and 3.40 MeV ($\frac{9}{2}^+$) in ^{25}Mg are weakly populated in (d, p) reactions [18]) and are assumed to be weak in this case too.

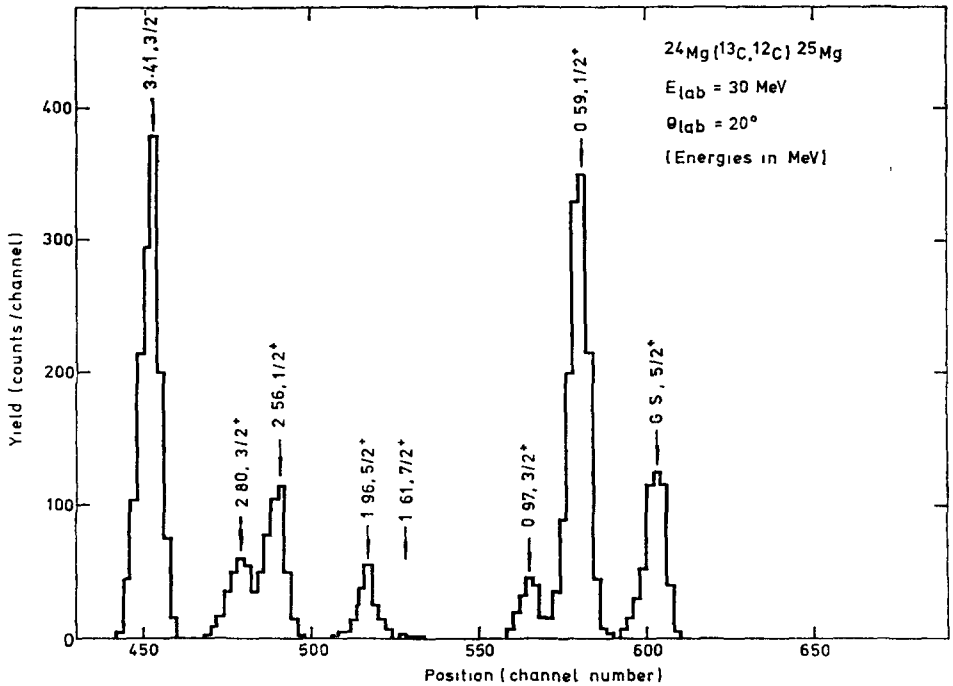

Fig. 1 Position spectrum for $^{12}C(6^+)$ ions from the $^{24}Mg(^{13}C, ^{12}C)^{25}Mg$ reaction at 30 MeV incident energy.

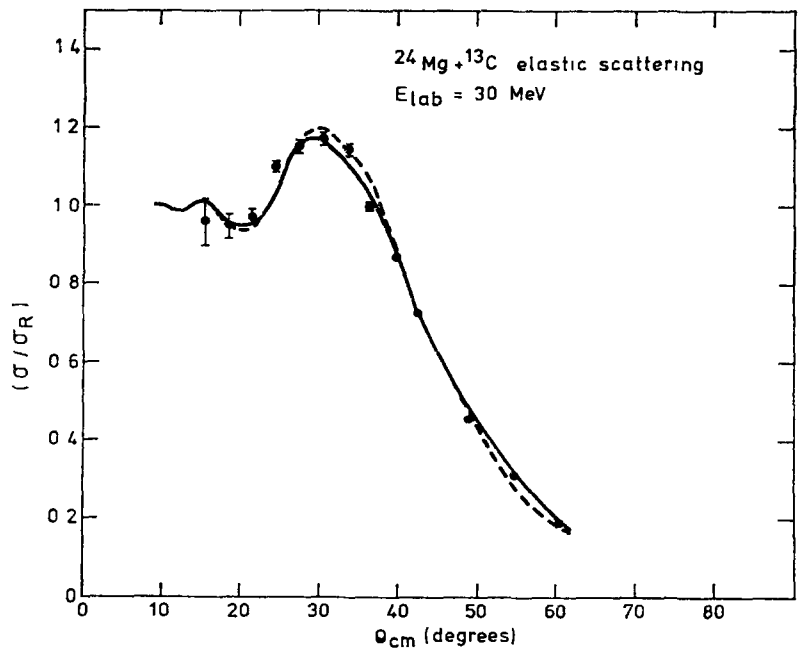

Fig. 2. Differential cross section normalised to Rutherford for the elastic scattering of ^{13}C from ^{24}Mg at 30 MeV. The solid and dashed lines are theoretical predictions from potentials A and B respectively.

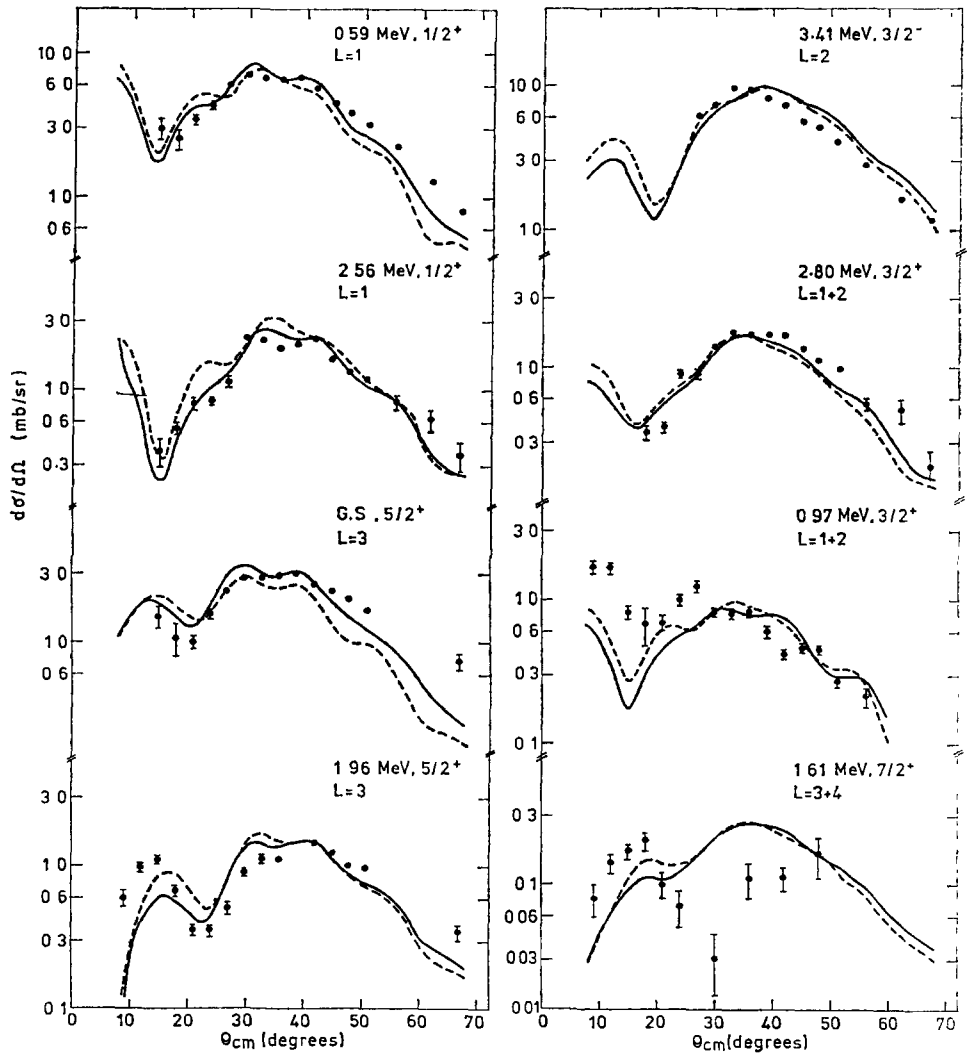

Fig. 3. Angular distributions from the $^{24}Mg(^{13}C, ^{12}C)^{25}Mg$ reaction at 30 MeV incident energy. The solid and dashed lines are theoretical DWBA predictions from potentials A and B respectively

Measurements of both elastic scattering and reaction cross sections were taken at a number of angles between 6° and 46° (lab) with respect to the beam axis. Relative normalisation between angles was accomplished by simultaneously recording an energy spectrum in a surface-barrier monitor detector placed at a fixed angle. An absolute cross section was obtained by comparing the reaction yield to measurements of the elastic yield at forward angles where the cross section approaches the Rutherford value. This method lead to an accuracy of about $\pm 15\,\%$. The yield was also corrected

for the variation in the 6^+ charge state fraction [19]) of the emerging ions. The fraction varies smoothly and continuously between 0.6 and 0.8 over the angular range covered.

Measured angular distributions for the elastic scattering and the (^{13}C, ^{12}C) reaction are shown in figs. 2 and 3 respectively. The solid and dashed lines are theoretical predictions and are discussed in the following section. Peak fitting was carried out to extract the yields of the 2.56-2.80 MeV doublet and the yield of the 0.97 MeV peak which is on the tail of the 0.59 MeV peak. Although not indicated in fig. 3, most of the data points have been measured more than once in separate runs and the agreement in all cases was satisfactory. Forward angle data for the ground state and 0.59 MeV levels were not obtained due to the count rate problems arising from the presence of elastically scattered ^{13}C ions. For levels above 1.96 MeV excitation, reaction products from target impurities (carbon and oxygen) obscured the data at some forward angles.

3. Data analysis

3.1. ELASTIC SCATTERING

Before attempting to analyse the transfer data using the DWBA, it is necessary to determine some acceptable optical model parameters from the elastic scattering data. This has been done using the optical model search routine ABACUS [20]). For strongly absorbing particles it is well known that the elastic scattering is sensitive

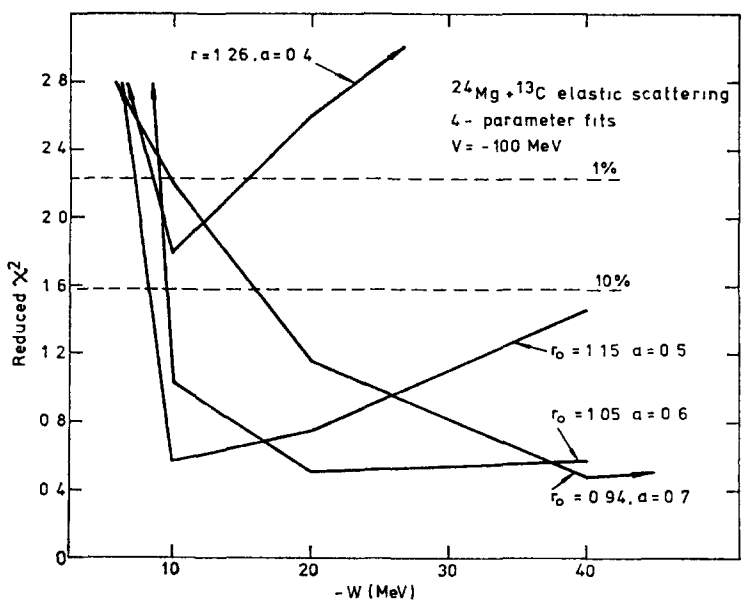

Fig. 4. Results of fitting the elastic scattering data to different families of four-parameter Woods-Saxon potentials. The dashed lines represent confidence levels of 10 % and 1 % as indicated.

only to the tail of the potential, giving rise to the Igo ambiguity [21]). For this reason it was decided to start by using a four-parameter Woods-Saxon potential well of the volume type, with the real and imaginary geometries constrained to be the same. The procedure was to fix arbitrarily the real depth V equal to -100 MeV and then for discrete values of the imaginary depth W and diffuseness a, search on the radius r_0. The results of such a procedure are shown in fig. 4 where the reduced χ^2 gives a measure of the goodness of fit and the dotted lines correspond to the 10 % and 1 % confidence levels. Within our parameterisation the elastic data seem to suggest only that $a \gtrapprox 0.4$ and that W is deeper than about -10 MeV. As noted for example by Satchler [22]), the one quantity that is well determined is the value of the real potential close to the strong absorption radius. All of the potentials indicated in fig. 4 give $l = 14\hbar$ for the angular momentum at which the transmission coefficient falls to a half, giving a value of 8.3 fm for this radius using a classical orbit relationship, whereas the real parts of the potentials all have the value of -0.4 MeV at a radius of 8.8 fm. It is clear that the imaginary potential is rather poorly determined. In a study of the energy dependence of the optical potential for the scattering of ^{16}O from ^{58}Ni, Satchler [23]) found that the ratio of imaginary to real well depth increased from roughly 0.1 at the Coulomb barrier to roughly 0.5 at 50 % above the barrier. For the bombarding energy used here, the above would suggest an imaginary well depth in the neighbourhood of -30 MeV.

3.2. TRANSFER REACTION

The analysis of the transfer data was carried out using the single-step, exact finite range, DWBA code LOLA [24]). Initially the optical potentials indicated in fig. 4 with a depth of $W = -30$ MeV were tried. These potentials achieved a reasonable fit to the bell-shaped angular distributions and the fits were essentially the same regardless of which geometry (r_0 and a) was used. However it was found that while a forward angle peak for the 1.96 MeV angular distribution is indeed predicted, the magnitude of this peak was considerably underestimated. By reducing the absorption to $W = -10$ MeV it was possible to enhance this part of the cross section although not by a large enough factor. Any further reduction in W produced oscillations in the whole of the angular distribution which were incompatible with the data, as well as unacceptable fits to the elastic scattering (fig. 4). Such a sensitivity of the forward angle cross section to the imaginary part of the potential has been reported by other authors [9, 12]). For comparison with the data we have chosen two potentials with $W = -10$ MeV and geometries of r_0, $a = 1.15, 0.5$ and r_0, $a = 1.05, 0.6$ respectively. Details of the parameters used in the calculation are given in table 1. The parameters r_c and λ are Coulomb radius and Thomas spin-orbit factor respectively.

Transitions to the $J^\pi = \frac{1}{2}^+$ states at 0.59 and 2.56 MeV proceed solely via $L = 1$ transfer. The DWBA prediction for the 2.56 MeV state is quite reasonable, while the 0.59 MeV angular distribution is somewhat underestimated at backward angles. This can be improved by increasing the depth of the imaginary potential for this state

TABLE 1

Parameters used in the DWBA analysis

	V (MeV)	r_V (fm)	a_V (fm)	W (MeV)	r_W (fm)	a_W (fm)	r_c (fm)	λ
Potential A [a])	−100	1.15	0.5	−10	1.15	0.5	1.25	0
Potential B [a])	−100	1.05	0.6	−10	1.05	0.6	1.25	0
Bound states		1.25	0.65				1.25	25
l-values	0–41							
Integration	0–20 fm in 0.1 fm steps							
Kernel width	3.0 fm							

a) Same optical parameters in incident and exit channels. $R_{V,W} = r_{V,W}\,(A_1^{\frac{1}{3}}+A_2^{\frac{1}{3}})$.

Transitions to the $J^\pi = \frac{3}{2}^+$ states at 0.97 and 2.80 MeV proceed mainly via $L = 1$ transfer, the non-normal $L = 2$ transfer allowed by recoil contributing about 20 % to the theoretical cross section. The fit for the 2.80 MeV state is good, but the dramatic change in the shape of the angular distribution seen for the 0.97 MeV state is not reproduced at all by the DWBA. This discrepancy appears to be similar in character to those reported by Ball *et al.* [12]) in their study of the ^{26}Mg(^{16}O, ^{15}N) and ^{30}Si(^{16}O, ^{15}N) reactions at 45 MeV. Transitions to the $J^\pi = \frac{5}{2}^+$ states at 0.0 and 1.96 MeV proceed via $L = 3$ transfer, the predicted non-normal $L = 2$ component being small in this case. The fit for the 1.96 MeV state reproduces quite well the data around the grazing peak and the position of the forward peak, but it was not possible to reproduce the magnitude of the forward peak within the present parameterisation. It can be seen that the potential with $r_0, a = 1.05, 0.6$ does better at forward angles, presumably because the larger diffuseness means a lower level of absorption inside the strong absorption radius. The fit for the 0.0 MeV state is underestimated at backward angles and the data do not extend far enough forward to test the predictions in this region. The transition to the $J^\pi = \frac{3}{2}^-$ state at 3.41 MeV proceeds via an $L = 2$ transfer, the predicted non-normal $L = 1$ component being small. Although the overall shape of the angular distribution agrees with the data, there appears to be a shift of about 4° between theory and experiment.

A direct transition to the $J^\pi = \frac{7}{2}^+$ state would proceed via an $L = 3$ transfer with the theoretical non-normal $L = 4$ transfer contributing about 20 % to the cross section. In this case the DWBA prediction bears no resemblance to the data, a fact which is hardly surprising in view of the small theoretical spectroscopic factor for this level [25]), and the failure of the DWBA to fit the data obtained from the ^{24}Mg(d, p) reaction [15, 16]).

A comparison of the spectroscopic factors obtained in this experiment with the results from (d, p) work and theoretical calculations using the Nilsson model is given in table 2. Apart from the 1.61 MeV level which is far too strongly populated to proceed via a direct transfer, the agreement is within the usual uncertainties en-

TABLE 2

Spectroscopic factors associated with ^{25}Mg levels

E_x (MeV)	J^π	Assumed config.	Present work		(d, p) [a]		Theor. ref. [25])
			potl. A	potl. B	ref. [15])	ref. [16])	
0.0	$\frac{5}{2}^+$	$1d_{\frac{5}{2}}$	0.23	0.14	0.32	0.29	0.33
0.59	$\frac{1}{2}^+$	$2s_{\frac{1}{2}}$	0.44	0.40	0.45	0.42	0.30
0.97	$\frac{3}{2}^+$	$1d_{\frac{3}{2}}$	0.30	0.24	0.35	0.24	0.25
1.61	$\frac{7}{2}^+$	$1g_{\frac{7}{2}}$	0.59	0.49			0.0005
1.96	$\frac{5}{2}^+$	$1d_{\frac{5}{2}}$	0.07	0.06	0.11	0.06	0.06
2.56	$\frac{1}{2}^+$	$2s_{\frac{1}{2}}$	0.11	0.10	0.11		
2.80	$\frac{3}{2}^+$	$1d_{\frac{3}{2}}$	0.33	0.25	0.34		
3.41	$\frac{3}{2}^-$	$2p_{\frac{3}{2}}$	0.22	0.18		0.25	

[a]) Same bound state parameters used as quoted in table 1.

countered in DWBA analysis. The fits for the angular distributions (with the exception of the 0.97, 1.61 and 1.96 MeV levels) could probably be further improved by a wider search for optical model potentials, or by optimising the fit for each transition individually. The necessity for doing so may, of course, reflect the presence of higher order processes in these transitions. More serious however is the inability of the DWBA to predict the magnitude of the forward angle peak in the 1.96 MeV distribution, the change in the type of angular distribution between the 2.80 MeV and 0.97 MeV $\frac{3}{2}^+$ states, and the shape and magnitude of the 1.61 MeV distribution.

4. Discussion

Following the treatment of Kahana *et al.* [1]), the most forward peak in the angular distribution of a heavy-ion induced reaction is expected to fall at an angle (θ_M) satisfying the relationship

$$(M(M+2))^{\frac{1}{2}} < (l_0+\tfrac{1}{2})\theta_M < (2M(M+1))^{\frac{1}{2}}, \qquad (1)$$

where l_0 is the grazing angular momentum and M is the substate ($|M| \leqq L$) of the L-transfer with respect to the beam axis. For well-matched reactions, and at a sufficiently high bombarding energy the $M = \pm L$ substate is expected [1]) to dominate the differential cross section, and this in turn gives an L-dependence in the position of the most forward peak. For the ^{24}Mg(^{13}C, ^{12}C)^{25}Mg reaction an examination of the reaction amplitudes $|\beta_L^M|$ for the 1.96 MeV, $L = 3$ transition shows the maximum amplitude at $l = 15$ with predicted values of $\beta_3^3 = 0.6$, $\beta_3^2 = 0.3$, $\beta_3^1 = 0.05$ and $\beta_3^0 = 0.2$. In contrast the predicted amplitudes for the 2.56 MeV, $L = 1$ transition are $\beta_1^1 = 0.9$ and $\beta_1^0 = 0.45$. Although the $\beta_L^{M=L}$ amplitudes are not completely dominant, they are certainly preferred. Using the relationship in (1) yields

$$15.3° < \theta_{M=3} < 19.4°; \quad 6.8° < \theta_{M=1} < 8.0°.$$

Comparison with the DWBA predictions in fig. 3 shows forward angle peaks at $\approx 16°$ ($L = 3$) and $\approx 7°$ ($L = 1$). Consequently the presence of a peak at about 15° in the angular distribution of the 1.96 MeV state can be understood in terms of a one-step direct reaction, but as discussed in the previous section it was not possible to predict the magnitude of this peak.

The marked difference between the angular distributions for the two $J^\pi = \frac{3}{2}^+$ states at 0.97 and 2.80 MeV provides an interesting comparison. Lemaire *et al.* [26]) have reported a similar effect present in the angular distributions measured in the ^{76}Ge(^{16}O, ^{14}C)^{78}Se reaction to the ground state and first excited 2^+ state. The change in the distribution from bell-shaped (ground state) to an oscillatory pattern with the cross section rising to forward angles (2^+ state) was accounted for by Tamura *et al.* [27]) with a coupled-channel calculation which included inelastic excitation in the exit channel. A more transparent explanation of the underlying reasons for these angular distributions has been given by Udagawa *et al.* [28]) using the semi-quantatitive model for heavy-ion reactions [1-3]). Following this treatment and considering only the $M = 0$ substate of the angular momentum transfer the reaction amplitude can be parameterised by

$$a_l = \exp(2i\delta_l) \exp[-(l-l_0)^2/\Gamma^2], \tag{2}$$

which reflects the localisation in l-space around the grazing angular momentum l_0. The phase is parameterised by assuming a linear variation around l_0 and writing

$$\psi = [\mathrm{d}(2\delta l)/\mathrm{d}l]_{l=l_0}. \tag{3}$$

For a heavy-ion reaction there is expected to be a close relation between ψ and the elastic phase shifts [28]). Using an asymptotic expression for the angular dependence of the transition amplitude leads to a cross section given by

$$\sigma_{M=0}(\theta) \propto \frac{1}{\sin\theta} |\exp\{-(\tfrac{1}{4}\Gamma^2)\,(\theta-\psi)^2\} \exp\{-i[(l_0+\tfrac{1}{2})\theta-\tfrac{1}{4}\pi]\} + \exp\{-(\tfrac{1}{4}\Gamma^2)\,(\theta+\psi)^2\} \exp\{i[(l_0+\tfrac{1}{2})\theta-\tfrac{1}{4}\pi]\}|^2 \tag{4}$$

Large forward angle cross sections and oscillations occur when Γ and/or ψ are small. For the ^{76}Ge(^{16}O, ^{14}C)^{78}Se reaction, Udagawa *et al.* [28]) show that the anomalous (non-bell shaped) distribution for the 2^+ state occurs because $\psi(2^+)$ is significantly smaller than ψ (ground state). They also show that this arises because $\psi(2^+)$ is closely related to inelastic phase shifts whereas ψ(ground state) is related to the elastic phase shifts. An application of this type of analysis to the two $J^\pi = \frac{3}{2}^+$ transitions observed in the present work is shown in fig. 5. It can be seen that the trend of the data can be reproduced by choosing $\psi = 42°$ for the 2.80 MeV state and $\psi = 30°$ for the 0.97 MeV state. The parameters $l_0 = 15$ and $\Gamma = 4.0$ have been chosen so that they approximate the DWBA predictions for the reaction amplitudes of the 2.80 MeV angular distribution. The dashed lines on fig. 5 show that a slightly better fit to the data can be obtained by small variations in Γ. Consequently we believe that the non-

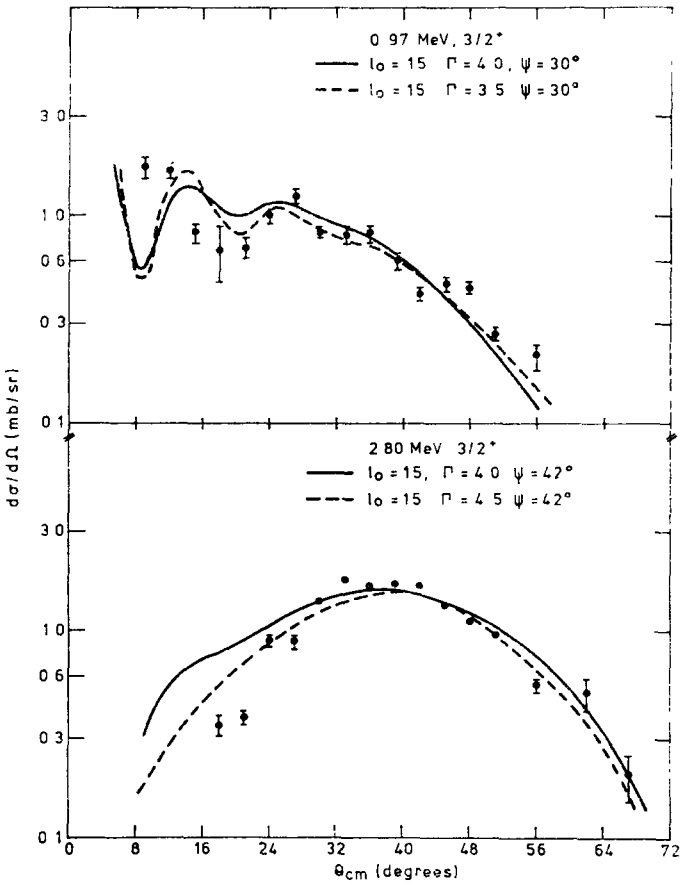

Fig. 5. The ^{24}Mg(^{13}C, ^{12}C)^{25}Mg reaction. Comparison of the experimental angular distributions of the $\frac{3}{2}^+$ states at 0.97 and 2.80 MeV with the predictions of the semi-quantitative model

bell-shaped angular distribution for the 0.97 MeV state is evidence of the coupling of inelastic processes in the transition to this state.

The angular distribution for the 1.61 MeV state has a very unusual shape, displaying a deep minimum located at the grazing angle. This type of distribution is often seen in heavy-ion inelastic scattering, and arises because of the interference between nuclear and Coulomb scattering. The 1.61 MeV state in ^{25}Mg is the $\frac{7}{2}^+$ member of the $\frac{5}{2}^+(202)$ ground-state rotational band. The spectroscopic factor is small [25]), but there is a strong electric quadrupole transition connecting it to the ground state. Therefore the population of this state in the (^{13}C, ^{12}C) reaction might be expected to proceed almost exclusively by a transfer to the ground state followed by inelastic excitation of the 1.61 MeV state by the outgoing ^{12}C ejectile. Fig. 6 shows a comparison of the angular distribution for the 1.61 MeV state with a prediction of the differential cross section for the ^{25}Mg(^{12}C, ^{12}C)^{25}Mg(1.61 MeV) inelastic excitation

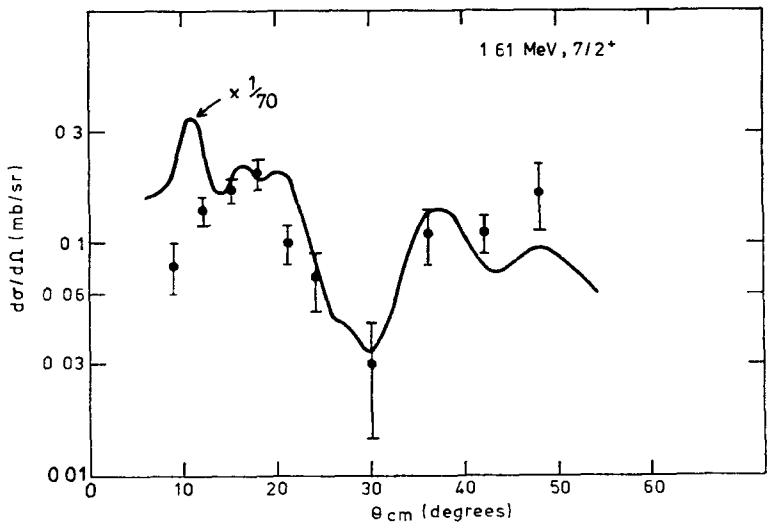

Fig. 6. The ^{24}Mg(^{13}C, ^{12}C)^{25}Mg reaction. Comparison of the experimental angular distribution of the $\frac{7}{2}^+$ state at 1.61 MeV with the prediction for inelastic excitation to this state. The theoretical cross section has been multiplied by a factor of $\frac{1}{70}$ to give it the same absolute value as the data.

of this state. The theoretical cross section has been multiplied by a factor of $\frac{1}{70}$ in order to normalise it to the data. The magnitude of the normalisation is not suprising in the absence of the full coupled-channel calculation. The calculation was carried out using the code DWUCK [29]) with a collective form factor and the potential set A from table 1. A nuclear deformation of $\beta^N = 0.5$ derived from the quadrupole moment of the ^{25}Mg ground state [30]) was used together with a value of $B(E2, \frac{5}{2}^+ \rightarrow \frac{7}{2}^+ = 1.8 \times 10^{-50} e^2 \cdot \mathrm{cm}^4$) derived from the lifetime and mixing ratio of the 1.61 MeV γ-ray transition [18]). It can be seen that the position and depth of the interference minimum is well reproduced by this first-order calculation. Consequently we suggest that the population of this state occurs predominantly through transfer followed by inelastic excitation, and that the angular distribution clearly shows the influence of the indirect Coulomb excitation on the transfer cross section. The first such evidence for the importance of Coulomb excitation was reported recently by Erb *et al.* [31]) in their study of the ^{186}W(^{12}C, ^{14}C)^{184}W reaction.

5. Summary

The one-step DWBA analysis of the (^{13}C, ^{12}C) transfer data obtained with the ^{24}Mg target has been successful in fitting the bell-shaped angular distributions and yielding spectroscopic factors in reasonable agreement with the light-ion work. The fits to the angular distributions could probably be improved further by a wider search for optical model parameters, or by optimising the fit for each transition individually. The necessity for individual optimisation of the parameters for each state may reflect the presence of higher order processes in these transitions.

The DWBA analysis has failed to predict the magnitude of the forward angle peak in the angular distribution for the $\frac{5}{2}^+$ state at 1.96 MeV although using the treatment of Kahana *et al.* [1]), the presence of the peak at 15° can be understood in terms of a one-step direct reaction. The angular distribution for the $\frac{3}{2}^+$ state at 0.97 MeV is quite different from the bell-shaped distribution measured for another $\frac{3}{2}^+$ state at 2.80 MeV. Using the semi-quantiative model for heavy-ion reactions [1, 2, 3]) it is possible to show that the departure from the bell-shaped angular distribution could be due to the coupling of inelastic processes in the transition to the state at 0.97 MeV.

The angular distribution for the $\frac{7}{2}^+$ state at 1.61 MeV displays an unusual shape with a deep minimum at the grazing angle. This shape is reminiscent of the heavy-ion inelastic scattering and arises because of the interference between the nuclear and Coulomb scattering. The differential cross section for the inelastic excitation of the 1.61 MeV state has been calculated using DWUCK [29]) and the position and depth of the interference minimum have been reproduced well. The calculations suggest that the population of the $\frac{7}{2}^+$ state at 1.61 MeV occurs predominantly through transfer followed by inelastic excitation.

Thanks are due to the staff of the Harwell Tandem accelerator for their assistance. The authors wish to thank Prof. G. C. Morrison for advice and support in this work and Drs. A. T. G. Ferguson and B. Rose for helpful suggestions in the final draft. One of us (N.E.S.) wishes to acknowledge a grant from the Science Research Council.

References

1) S. Kahana, P. D. Bond and C. Chasman, Phys. Lett. **50B** (1974) 199
2) V. M. Strutinsky, JETP (Sov. Phys.) **19** (1964) 1401
3) W. E. Frahn and R. H. Venter, Nucl. Phys. **A59** (1964) 651
4) P. R. Christensen, O. Hansen, J. S. Larsen, D. Sinclair and F. Videbæk, Phys. Lett. **45B** (1973) 1074
5) P. D. Bond, J. D. Garrett, O. Hansen, S Kahana, M. J. LeVine and A. Z. Schwarzschild, Phys Lett. **47B** (1973) 231
6) M. J. LeVine, A. J. Baltz, P. D. Bond, J. D. Garrett, S. Kahana and C. E Thorn, Phys. Rev. **C10** (1974) 1602
7) M. J. Schneider, C. Chasman, E. H. Auerbach, A. J. Baltz and S. Kahana, Phys. Rev. Lett. **31** (1973) 320
8) W. Henning, D. G. Kovar, B. Zeidman and J. R. Erskine, Phys. Rev. Lett. **32** (1974) 1015
9) A. J. Baltz, P. D. Bond, J. D. Garrett and S. Kahana, Phys. Rev. **C12** (1975) 136
10) P. D. Bond, C. Chasman, J. D. Garrett, C. K. Gelbke, O. Hansen, M. J. LeVine, A. Z. Schwarzschild and C. E. Thorn, Phys. Rev. Lett. **36** (1976) 300
11) W. Henning, D. G. Kovar, J. R. Erskine and L. R. Greenwood, Phys. Lett. **55B** (1975) 49
12) J. B. Ball, O. Hansen, J. S. Larsen, D. Sinclair and F. Videbæk, Nucl. Phys. **A244** (1975) 341
13) T. Tamura, K. S. Low and T. Udagawa, Phys. Lett. **51B** (1974) 116
14) K. Yagi, D. L. Hendrie, L. Kraus, C. F. Maguire, J. Mahoney D. K. Scott, Y. Terrien, T. Udagawa, K. S. Low and T. Tamura, Phys. Rev. Lett. **34** (1975) 96
15) U. Schieb, A Hofmann, G. Philipp and F. Vogler, Nucl. Phys. **A203** (1973) 177
16) T. A. Schmick, K. W. Kemper, P. K Bindal and R. D. Koshel, Phys. Rev. **C10** (1974) 556

17) B. W. Hooton, Harwell Report, AERE-M2637 (1974)
18) P. M. Endt and C. van der Leun, Nucl. Phys. **A214** (1973) 1
19) J. B. Marion and F. C. Young, Nuclear reaction analysis (North-Holland, Amsterdam, 1968) p. 41
20) E. H. Auerbach, Brookhaven National Laboratory, Report No. BNL-6562
21) G. Igo, Phys. Rev. **115** (1959) 1665
22) G. R. Satchler, Phys. Lett. **55B** (1975) 167
23) G. R. Satchler, Phys. Lett. **58B** (1975) 408
24) R. DeVries, Phys. Rev. **C8** (1973) 951
25) D. Dehnhard and J. L. Yntema, Phys. Rev. **160** (1967) 964
26) M. C. Lemaire, M. C. Mermaz, H. Aztark and H. Cunsolo, Phys. Rev. **C10** (1974) 1103
27) T. Tamura, K. S. Low and T. Udagawa, Phys. Lett. **51B** (1974) 116
28) T. Udagawa and T. Tamura, Phys. Lett. **57B** (1975) 135
29) P. D. Kunz, University of Colorado, 1967, unpublished
30) K. Nakai, F. S. Stephens and R. M. Diamond, Phys. Lett. **34B** (1971) 389
31) K. A. Erb, D. L. Hanson, R. J. Ascuitto, B. Sørensen, J. S. Vaagan and J. J. Kolata, Phys. Rev. Lett. **33** (1974) 1102